End Cell Shielding and Streaming Analysis of MARS Tandem Mirror Reactor

Laila A. El-Guebaly

February 1985

UWFDM-621

Presented at the Sixth Topical Meeting on the Technology of Fusion Energy, San Francisco, CA, 3-7 March 1985; Fusion Tech. 8, No. 1, Part 2B, 1043 (July 1985).

FUSION TECHNOLOGY INSTITUTE

UNIVERSITY OF WISCONSIN

MADISON WISCONSIN

End Cell Shielding and Streaming Analysis of MARS Tandem Mirror Reactor

Laila A. El-Guebaly

Fusion Technology Institute
University of Wisconsin
1500 Engineering Drive
Madison, WI 53706

http://fti.neep.wisc.edu

February 1985

UWFDM-621

Presented at the Sixth Topical Meeting on the Technology of Fusion Energy, San Francisco, CA, 3-7 March 1985; Fusion Tech. 8, No. 1, Part 2B, 1043 (July 1985).

END CELL SHIELDING AND STREAMING ANALYSIS OF MARS TANDEM MIRROR REACTOR

LAILA A. EL-GUEBALY, Fusion Technology Institute
University of Wisconsin, 1500 Johnson Drive
Madison, WI 53706
(608) 263-1623

ABSTRACT

In recent studies of tandem mirror reactors some attention has been focused on the problems associated with radiation streaming into penetrations of both the central fusion chamber and the end cells. This work presents the radiation analysis for the end cells of the commercial tandem mirror reactor MARS. The amount of radiation streaming into the penetrations was quantified and the radiation problems at the direct convertor were analyzed.

INTRODUCTION

The problem of radiation in penetrations has been recognized for some time in tokamak studies. In a tandem mirror power reactor design the problem appears to be less severe since the only penetrations of the central fusion chamber are the openings to the end cells. Considerable amounts of neutrons are generated in the end cells and the streaming of these neutrons through the penetrations reduces the effectiveness of the bulk shield and presents a variety of shielding and maintenance problems to the designers as the sensitive components located at the back of these penetrations are subject to damage by radiation. Fortunately, in most TMR designs the end cell penetrations are not in direct line of sight of the central cell source neutrons. Hence, the neutron source in the end cell dominates the streaming problem and the problem of neutron streaming from the central cell to the end cell only concerns the leakage to the ends of the reactor where the direct convertors are located. Substantial work[2-6] during the past ten years uncovered the severity of the penetration problems. Some problems can be solved by introducing a radiation shield and extending it to the back of the penetration to protect the various components, but the main constraints could be the space limitations and the interference of the shield with a desirable arrangement of the components.

The 130 m long central cell of MARS[1] produces 2600 MW of fusion power in steady state and has a neutron wall loading of 4.3 MW/m^2. Other blanket features include the use of HT-9 for structural material and $Li_{17}Pb_{83}$ as the breeder and coolant. There is a high field choke coil at each end of the central cell, followed by a series of six C-shaped coils. Small copper insert coils (0.6 m bore) are used to boost the choke coil fields to 24 T. The direct conversion of the energy of the particles which leak out of both ends of the machine is accomplished by compact, gridless direct convertors which supply all the plant auxiliary power (~ 300 MWe). The end cell (40 m long) includes the transition, anchor, plug, recirculatizer, and direct convertor regions. It consists of the C coils and their shield and support structure, penetrations for the neutral beam injector (NBI) and ion and electron cyclotron resonance heating (ICRH and ECRH), neutral beam dumps, and the ion and electron thermal dumps at the direct convertor collector plates.

The general objectives of this study are to 1) analyze the streaming problems in the end cell, 2) provide radiation sources at the penetration entrances to be used in later modeling of the ducts themselves, and 3) investigate the possibility of simple disposal of radioactive waste of the direct convertor collector plates.

END CELL STREAMING ANALYSIS

Our interest here is centered on the radiation streaming through the end cell penetrations. This is of great importance in assessing the radiation effects in these penetrations. Evaluation of the radiation streaming through the ducts requires an accurate knowledge of the neutron source and the geometrical configuration of the shield as well as the size of the ducts. The linear neutron source distribution from the midplane of the choke coils to the end of the machine is shown in Fig. 1 along with the axial variation of the peak neutron wall loading. They are characterized by two relative peaks which drop to a negligible value near the end of the plug region. Figure 2 illustrates the end cell shield wall which closely follows the plasma boundary and allows for the required

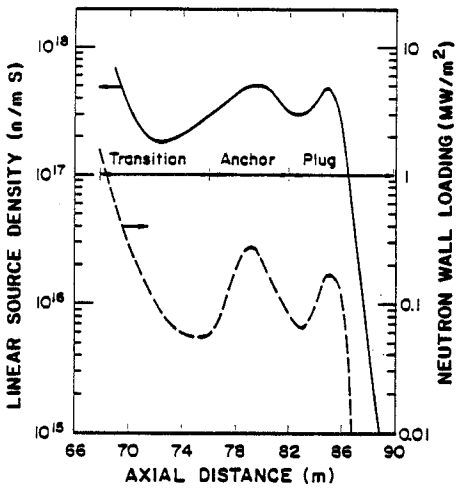

Fig. 1. Axial variation of the neutron source strength and wall loading in the end cell (the axial distance is measured from the midplane of the reactor).

spacing for the halo region. The plasma is circular up to the midplane of the choke coils and has an elliptical shape with varying ellipticity in the end cell. From the parametric study of the end cell shielding materials, the Fe1422/B_4C/H_2O shield was dictated as the best for meeting the combined criteria of low cost and adequate magnet protection. The ~ 0.5 m thick shield used in the end cell results in acceptable values for the damage in the C coils.

A. Calculational Model

To deal with the three-dimensional (3-D) geometrical configuration of the shield, the Monte Carlo code MCNP[1] and its RMCCS cross section library were used for the treatment of the streaming problem. The end cell shield and penetrations were modeled for the code and an effort was made to minimize the geometrical approximations of the shield. Figure 3 shows elevation and plan views of the model from the midplane of the choke coils to the end of the reactor. The figure illustrates the geometrical relationship of the ducts to the reactor. The axial locations and the sizes of the various penetrations are given in detail in Table I. The plasma boundary is not shown in the figure and the vertical lines are only used to define the regions for the code. Nominally, 0.5 m of shield is used in the end cell except at z positions in the range 88.35 - 92.35 m where the shield thickness is reduced to allow for the 0.64 m wide ECRH(B) ducts. There are no source neutrons in the recirculariser region. Nevertheless, a ~ 0.2 m thick shield is placed there to shield the plug-Yang and recirculariser coils against the streaming radiation from the reaction chamber.

B. Calculational Procedures and Results

The model shown in Fig. 3 was entered into the MCNP input to perform the 3-D neutronics and photonics calculations of the streaming problem. Trapping surfaces were located at the duct entrance surfaces* to count all crossing particles according to angle and energy bins. This information was then stored to serve as surface sources in later modeling of the ducts themselves.

The end cell penetrations are not in direct line of sight of the central cell source neutrons. Hence, the neutron source in the end cell dominates the streaming problem. A run of 50,000 histories was sampled isotropically from axial positions in the range 67.85 m to 90 m, according to the actual plasma shape (Fig. 2) and axial neutron source distribution (Fig. 1). Normalization of the source was such as to represent a neutron source of 7 x 10^{18} n/s. This source corresponds to a fusion power of 19.7 MW (at 17.6 MeV/fusion) for each end cell.

The number of particles crossing each trapping surface is given in Table II on a per second basis along with their associated relative standard deviations that range from 7 to 17% for neutrons and 20 to 61% for gamma rays. The NBI duct is the most severe case as is

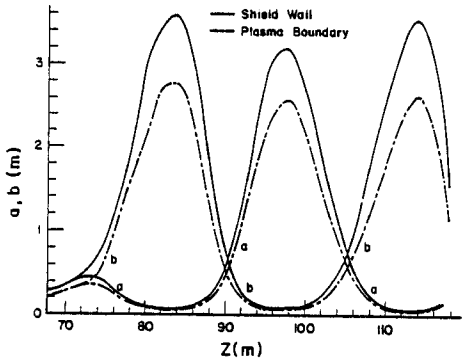

Fig. 2. Axial variation of the elliptical plasma surface and first wall semidiameters a and b.

*For the ECRH ducts, where the entrances consist of the intersection of several surfaces, the trapping surfaces are located behind the duct entrances.

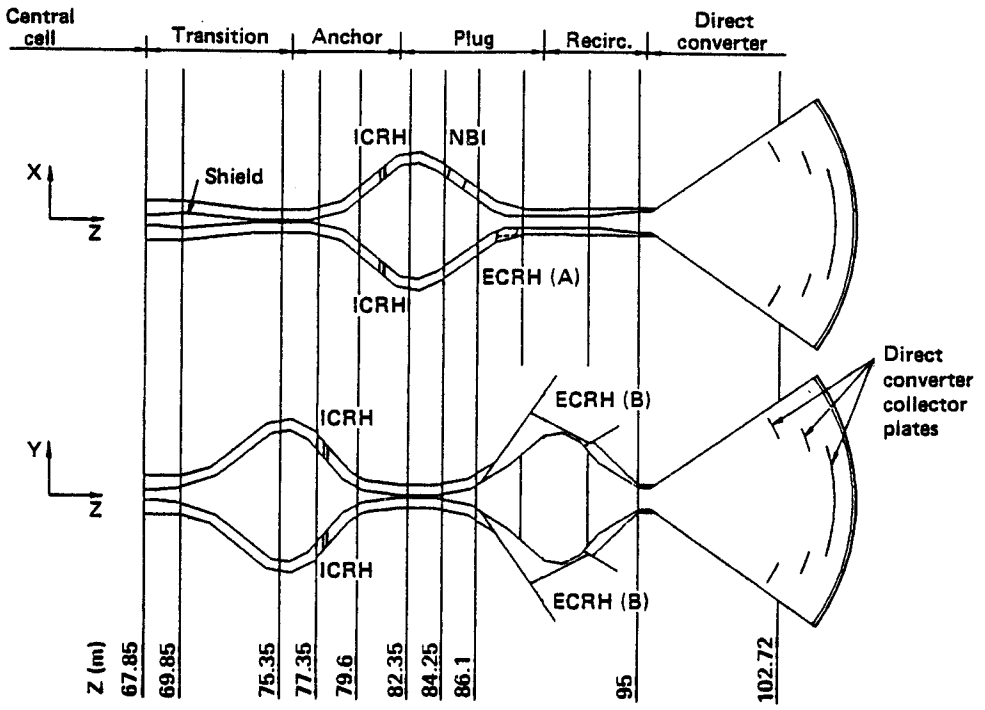

Fig. 3. Elevation and plan views of MARS end cell shield (output from MCNP plotting routine).

Table I. End Cell Penetrations

Duct	# per end	Location	Z* (m)	Size (m)	Injection angle
NBI	1	Plug	84.35	0.8 x 0.3	76°
ICRH	4	Anchor	77.85, 80.85	.232 dia.	90°
ECRH (B)	2	Plug	85.85 - 87.35	1.5 x 0.64 (at z axis)	55° - 31°
ECRH (A)	1	Plug	88.37 - 89.33	0.96 x 0.64	74° - 81°

*Intersection of the beam centerline with the plasma axis except for ECRH where the duct wall intersection is given.

evident by observation of the energy current density in the right hand column of the tabulated results. The energy spectra for particles crossing the trapping surface of the NBI are presented in Fig. 4 and show that approximately 25% of the crossing neutrons are source neutrons at 14.1 MeV. A significant number of lower energy secondary neutrons that have been moderated in and reflected from the shield also stream through the ducts, and ~ 70% of the neutrons have energies below 1 MeV. Inspection of the figure reveals that the angular distributions of the streaming particles peak at normal incidence to the trapping surface. This serves as a warning to carefully shield the NBI system in order to protect the vital components located at the back of the injector.

RADIATION ANALYSES FOR THE DIRECT CONVERTOR

Tandem mirror reactors require a large amount of recirculating power; the ability of the direct convertor (DC) to supply most (or all) of this power has the advantage of increasing the overall plant efficiency. Moreover, since this power becomes available as soon as

Table II. Radiation Streaming Through End Cell Penetrations

Duct*	Duct opening area (m^2)	Neutron/s	Gamma/s	Energy current density (MW/m^2)
NBI	0.24	2.204×10^{16}(±7%)	3.750×10^{15}(±20%)	6.194×10^{-2}
ECRH (A)	0.71	1.544×10^{16}(±9%)	2.564×10^{15}(±30%)	1.015×10^{-2}
ECRH (B-)	2.33	4.396×10^{15}(±17%)	5.60×10^{14}(±50%)	1.472×10^{-3}
ECRH (B+)	2.33	3.887×10^{15}(±17%)	7.761×10^{14}(±53%)	1.306×10^{-3}
ICRH (+x)	4.28×10^{-2}	6.398×10^{15}(±14%)	1.469×10^{15}(±37%)	7.665×10^{-2}
ICRH (-x)	4.28×10^{-2}	5.524×10^{15}(±15%)	6.124×10^{14}(±61%)	7.286×10^{-2}
ICRH (+y)	4.28×10^{-2}	6.378×10^{15}(±14%)	1.319×10^{15}(±39%)	8.977×10^{-2}
ICRH (-y)	4.28×10^{-2}	5.232×10^{15}(±15%)	1.755×10^{15}(±38%)	7.724×10^{-2}

*(+x) means duct at the positive x axis.

fusion takes place, it can supply power for startup before the turbines begin generating electricity. The end plasma technology is aimed at directly recovering as much energy as possible from the charged particles leaking from the hot core plasma and the cold halo region. The MARS design uses a new compact, gridless direct convertor which fits within the vacuum vessel of the end cell. As expected, the charged particles must be collected on surfaces designed to accept high heat fluxes (200-300 W/cm^2) without significant radiation damage. Also, the requirements for high water temperature (320°C) with high flow rate (>10 m/s) and low tritium permeation in the cooling water system forced consideration of the molybdenum alloy TZM as a candidate material for the DC collector plates and halo scrapers. However, the long lived activation products of molybdenum and the waste disposal of the collector plates caused some concern. This brought the need for neutronics and activation analysis for the DC collector plates to investigate the possibility of simple disposal of the radioactive waste.

A. Neutronics Analyses

The problem of neutron streaming from the reaction chamber to the direct convertor region was analyzed using the Monte Carlo code MCNP.[7] The calculational model is a duplicate of the model used before in the streaming study of the end cell penetrations. The neutron source, given in Fig. 1, was modeled from the midplane of the choke coil to the end of the plug region and sampled within the plasma boundary. To reduce the statistical error, the isotropic neutron source was directionally biased toward the direct convertor and the neutron weights were adjusted to reflect this variance reduction procedure. The homogeneous mixture used for the DC collector plates consisted of 95.5 vol.% molybdenum and 4.5 vol.% water. A run was made using 30,000 histories and the results were normalized to a total source of 7×10^{18} n/s. The calculations show that the values of the neutron fluxes at the inner collector, outer collector, and halo scraper are 5.09×10^{9} (± 7%), 4.78×10^{8} (± 12%), and 3.33×10^{8} (± 13%) n/cm^2 s, respectively. As anticipated, the inner collector has the highest flux as other plates are shielded from the direct neutron source. Editing of the results made use of the segmentation feature of MCNP. The 3 m radius inner collector was divided radially into 30 segments, each 0.1 m thick. The flux in each segment was printed and a plot of the results is given in Fig. 5. The flux peaks at the center of the plate and drops off radially toward the edge. The energy distribution of the neutron flux was also obtained and is presented in Fig. 6.

An attempt was made to analytically calculate the DC flux due to neutron streaming from the central cell based on several assumptions: 1) the neutron source is uniform across the plasma cross section; 2) only source neutrons are able to reach the DC as the choke coils attenuate the secondary neutrons generated in the blanket; and 3) the amount of neutron streaming into the DC is determined by the dimensions of the shield walls at the first two plasma fans closest to the central cell. The analytical results have shown that the average 14.1 MeV neutron flux over the inner collector plate is 4.94×10^{8} n/cm^2 s. The estimated radial distribution of this flux is shown in Fig. 5. This leads to a total flux at the inner collector plate of 5.59×10^{9} n/cm^2 s.

B. Activation Analyses

The activation analyses were carried out for the DC plates using the DKR[8] fusion reactor radioactivity calculation code and its associated data library. The analyses employ the neutron fluxes and energy spectra obtained from the MCNP run as described before. Two cases were considered with irradiation times of 12 and 24 FPY's and the results are given in Table III. The legal limits in this table are taken from

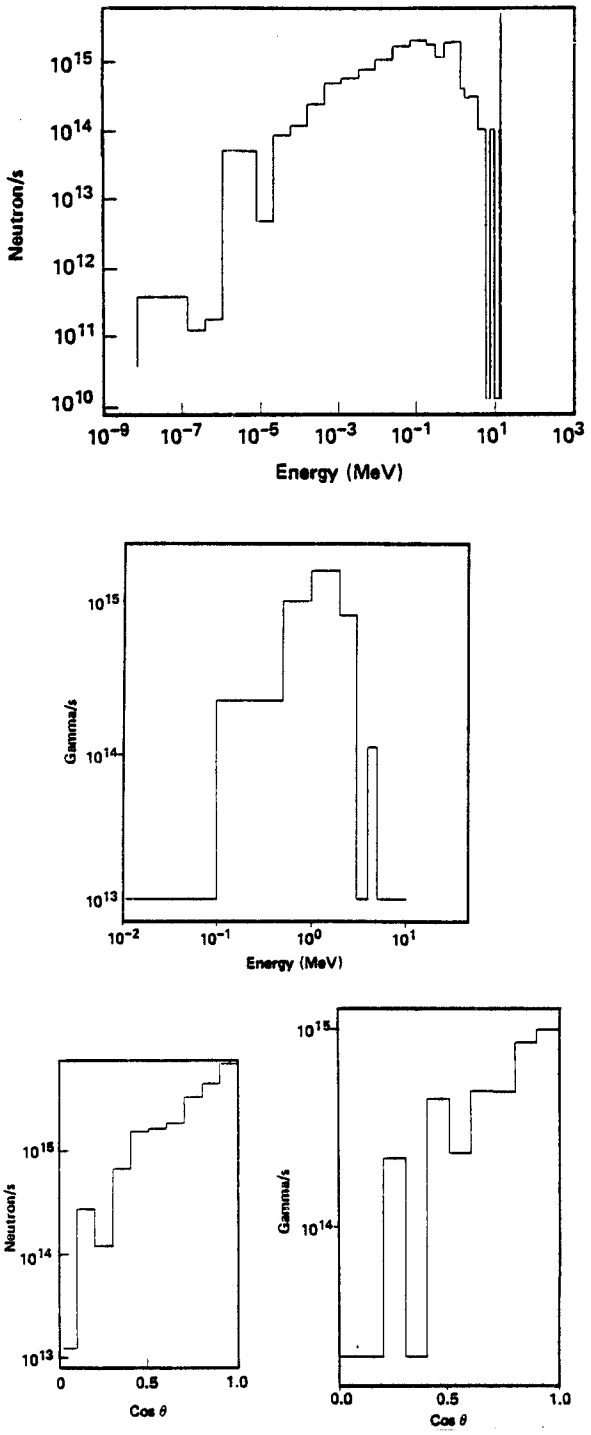

Fig. 4. Energy spectra and angular distribution of particles streaming through the NBI duct (θ is measured from the normal to the entering surface).

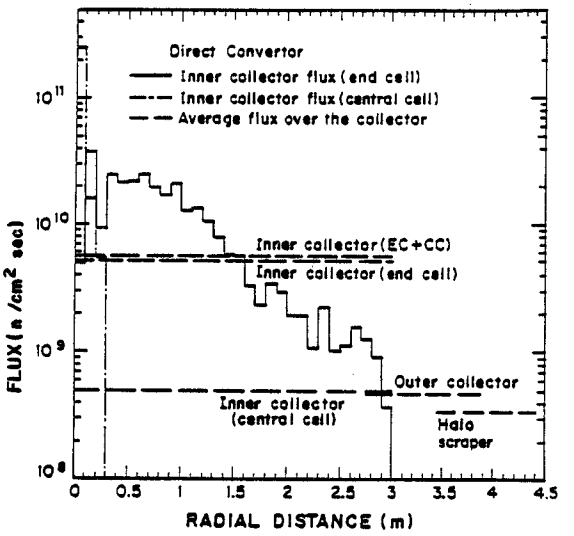

Fig. 5. Neutron flux at the direct convertor collector plates.

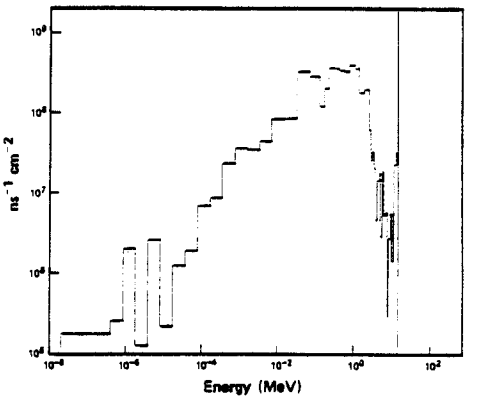

Fig. 6. Neutron energy spectrum for the inner collector plate.

10CFR61[9] or estimated from the data therein. The Waste Disposal Rating (WDR) serves as a guide to the designers in evaluating how easily a particular material can be disposed of. The WDR is the sum of the ratio of the specific activity to the maximum permissible concentration for the different isotopes. If the WDR>1, the material cannot be disposed of by near surface burial unless diluted. If 0.1 < WDR <1, the waste is termed low level Class C intruder waste. This waste must be packaged for near surface burial with the idea that it will still pose a hazard after the 100 year institu-

Table III. Specific Activities for Direct Convertor (Ci/m^3) - 12 and 24 FPY Irradiation Time

FPY	Isotope	Inner collector	Outer collector	Halo scraper	Class C legal limit	Fraction of legal limit
12	^{93}Mo	6.53×10^{0}	5.25×10^{-1}	3.72×10^{-1}	220	0.029
	^{94}Nb	7.50×10^{-3}	2.13×10^{-5}	3.54×10^{-5}	0.2	.0375
	^{99}Tc	5.20×10^{-3}	8.74×10^{-4}	6.61×10^{-4}	3	.0015
						WDR = .068
24	^{93}Mo	1.31×10^{1}	1.05×10^{0}	7.41×10^{-1}	220	0.059
	^{94}Nb	1.5×10^{-2}	4.25×10^{-5}	7.07×10^{-5}	0.2	.075
	^{99}Tc	1.04×10^{-2}	1.75×10^{-3}	1.33×10^{-3}	3	.003
						WDR = .137

tional period is over. If WDR < 0.1, the waste is Class A segregated waste. It must meet less stringent packaging and burial requirements.

Tabulated results show that the DC plates could be classified as Class A waste in the case of 12 FPY irradiation period and Class C for the 24 FPY period. However, in the latter case the waste could easily be converted to Class A by encasing the plates in concrete and increasing its volume by ~ 40%. Alternatively, the central portion of the inner collector could be removed and buried as Class C waste with the remainder of the inner collector, the outer collector, and the halo scraper disposed of as Class A.

CONCLUSIONS

The MARS end cell was modeled for radiation analysis using the Monte Carlo code MCNP. The calculations result in the amount of radiation at the penetration entrances and the neutron flux at the direct convertor collector plates. The inner collector has the highest flux of 5.6×10^{9} n/cm^2s, as the other plates are shielded from the direct neutron source. The subsequent activation analyses reveal that near surface burial of the DC collector plates is feasible. It is noteworthy that the neutron flux at the DC collector plates is relatively low so that bulk damage that is normally associated with such neutrons is probably not important but the sputtering problems of the energetic charged particles could be adverse unless properly handled. Also, the results indicated that the NBI duct has high energy current density (0.06 MW/m^2) at the entrance and this could be a source of difficulty unless additional shielding is introduced within the injector.

ACKNOWLEDGEMENTS

The author wishes to acknowledge helpful discussions with Professors Charles Maynard and William Vogelsang of the University of Wisconsin. She is also grateful to Andrew White for his assistance with the radioactivity calculations. This work was performed under the auspices of the United States Department of Energy.

REFERENCES

1. B.G. LOGAN et al., "Mirror Advanced Reactor Study - Final Report", UCRL-53480, Lawrence Livermore National Laboratory (1984).

2. M.M. RAGHEB and C.W. MAYNARD, Journal of Fusion Energy, 1, 367 (1981).

3. L.A. EL-GUEBALY and C. MAYNARD, Nucl. Technol./Fusion, 5, 101 (1984).

4. R.A. LILLIE, R.T. SANTORO, and R.G. ALSMILLER, JR., "Estimated Nuclear Effects in the Neutral Beam Injectors of a Large Fusion Reactor," ORNL/TM-7526, Oak Ridge National Laboratory (1980).

5. W.T. URBAN, "Neutron Streaming Through Straight and Single Bend Slots", LA-9761-MS, Los Alamos National Laboratory (1983).

6. M.M. RAGHEB, A.C. KLEIN, and C.W. MAYNARD, Nucl. Technol./Fusion, 1, 99 (1981).

7. Los Alamos National Laboratory Group X-6, "MCNP - A General Monte Carlo Code for Neutron and Photon Transport, Version - 2C," LA-7397-M, Los Alamos National Laboratory (1981).

8. T.Y. SUNG and W.F. VOGELSANG, "DKR: A Radioactivity Calculation Code for Fusion Reactors", UWFDM-170, University of Wisconsin Fusion Technology Institute (1976).

9. Code of Federal Regulation, "Licensing Requirements for Land Disposal of Radioactive Wastes", Vol. 47, #248, Chapter 10 (1982).